Structural and electrical properties of $PbMoO_4$ under high pressure

2007 J. Phys.: Condens. Matter 19 425215

(http://iopscience.iop.org/0953-8984/19/42/425215)

IOP PUBLISHING JOURNAL OF PHYSICS: CONDENSED MATTER

J. Phys.: Condens. Matter **19** (2007) 425215 (7pp) doi:10.1088/0953-8984/19/42/425215

Structural and electrical properties of $PbMoO_4$ under high pressure

Cuiling Yu[1], Qingjiang Yu[1], Chunxiao Gao[1,3], Bao Liu[1], Aimin Hao[1], Chunyuan He[1], Xiaowei Huang[1], Dongmei Zhang[1], Xiaoyan Cui[1], Dongmei Li[1], Hongwu Liu[1], Yanzhang Ma[2] and Guangtian Zou[1]

[1] State Key Laboratory of Superhard Materials, Institute of Atomic and Molecular Physics, Jilin University, Changchun 130012, People's Republic of China
[2] Department of Mechanical Engineering, Texas Tech University, Lubbock, TX 79409, USA

E-mail: cxgao599@yahoo.com.cn

Received 3 August 2007
Published 18 September 2007
Online at stacks.iop.org/JPhysCM/19/425215

Abstract

High pressure Raman spectra and *in situ* electrical conductivity measurement of scheelite-structure $PbMoO_4$ have been conducted using a diamond anvil cell (DAC). The Raman spectra of powdered $PbMoO_4$ were determined up to 26.5 GPa under nonhydrostatic conditions. The results indicate that $PbMoO_4$ undergoes a transition from crystal to amorphous phase with increasing pressure, and the phase-transition pressure was about 12.5 GPa. The electrical conductivity of $PbMoO_4$ as a function of pressure and temperature was studied using a designed DAC. The experimental results show that the electrical conductivity of $PbMoO_4$ increases with increasing pressure and temperature. Compared with the electrical conductivity value of $PbMoO_4$ at 7.4 GPa and 430 K, it increases by about two orders of magnitude at 26.5 GPa and 430 K.

1. Introduction

$PbMoO_4$ crystals belong to the tetragonal scheelite structure with point group symmetry $4/m$ and space group symmetry $I4_1/a$. It is a very important material for acousto-optic light deflector, modulator, adjustable filter and surface acoustic wave devices because of its high acousto-optic figure of merit, low optical loss in the region 420–3900 nm and favorable mechanical impedance for acoustic matching [1–8].

$PbMoO_4$ crystal has been a subject of intense research for over three decades. However, there are still fundamental questions concerning the electronic properties of $PbMoO_4$, especially concerning the nature of its structure. Raman studies on scheelite structure compounds under different pressures were carried out by Ganguly and Nicol, [9] who used the

[3] Author to whom any correspondence should be addressed.

modified Drickamer-type optical cell with NaCl as a pressure medium. They reported a phase transition to wolframite structure in $CaWO_4$ and $SrWO_4$ below 3 GPa by observing splittings of certain Raman peaks, but found no evidence for any phase transition in $PbMoO_4$. Subsequently, Jayaraman *et al* [10] studied the stability of scheelite-structure compounds under high pressure in a DAC with a 4:1 methanol ethanol mixture as the pressure medium. They investigated the structural stability of $PbMoO_4$ and $PbWO_4$ up to 12 GPa by Raman spectroscopy and found pressure-induced reversible phase transitions near 4.5 GPa for $PbWO_4$ and 9 GPa for $PbMoO_4$.

In addition, Van Loo [11] and Groenink [12] investigated the electrical conductivity of $PbMoO_4$ at different temperatures. The existence of charge carriers at high temperature and ionic majority defects in the oxygen sublattice were confirmed by conductivity measurements. Recently, Volnyanskiĭ *et al* [13] reported the dc and ac electrical conductivity of $PbMoO_4$ crystals in the temperature range from 300 to 550 K. Their results revealed the hopping mechanism of conduction in $PbMoO_4$ crystals. However, so far as we know, the electrical conductivity of $PbMoO_4$ under high pressure has not been investigated to date. In this work, the dc electrical conductivity of $PbMoO_4$ was measured accurately *in situ* using a microcircuit fabricated on a DAC based on the van der Pauw method. The results show that the electrical conductivity of $PbMoO_4$ increases with an increase in pressure and temperature. The effect of pressure on the electrical conductivity of $PbMoO_4$ is more obvious than that of temperature.

2. Experimental details

The Raman spectrum of the sample was measured in a DAC using a multifunction spectrum device (Jobin-Yvon Corporation, France, T64000) with a charge-coupled device (CCD) detector. The 488 nm line from an Ar/Kr ion laser was used. A Mao–Bell-type diamond anvil cell was utilized to generate high pressure, and the anvil culet was 400 μm in diameter with a bevel angle of 10°. Preindented T301 stainless steel was used as the gasket, and a ruby with a size of 2 μm was used as the pressure marker.

A convenient microcircuit was used to investigate the electrical conductivity of $PbMoO_4$. The manufacturing process of the microcircuit was similar to that described in our previous work [14, 15]. Firstly, a 0.3 μm-thick molybdenum (Mo) film was deposited on one diamond anvil (figure 1(b)) and then patterned into four detecting electrodes according to the van der Pauw model by photolithography and chemical etching (figure 1(c)). The distance between electrodes was 30 μm. To protect the Mo electrodes and to insulate them from the metal gasket under high pressure, a 2 μm-thick Al_2O_3 film was deposited on the Mo film (figure 1(d)). A detecting window was created in the center of the diamond culet and the electrodes were exposed by removing the Al_2O_3 layer using a chemical method to make the probes contact the sample (figure 1(e)). The configuration of the complete microcircuit is shown in figure 1(f). Figure 2 shows the cross section of the designed DAC device.

In electrical conductivity measurement, a 10 μA (I_1) direct current was first applied from A to B, and the voltage drop (V_1) between C and D was recorded. Then, the same current (named I_2) was applied from A to C, and the voltage drop (V_2) between B and D was recorded. The electrical resistivity was determined by the van der Pauw equation,

$$\exp(-\pi L R_A \sigma) + \exp(-\pi L R_B \sigma) = 1, \tag{1}$$

where R_A and R_B are the measured resistances ($R_A = V_1/I_1$, $R_B = V_2/I_2$), L is the thickness of the sample, and σ is the electrical conductivity. The thickness of the sample under pressure was determined by measuring the distance between the back facets of the two anvils with a modified micrometer having two symmetrical microprobes.

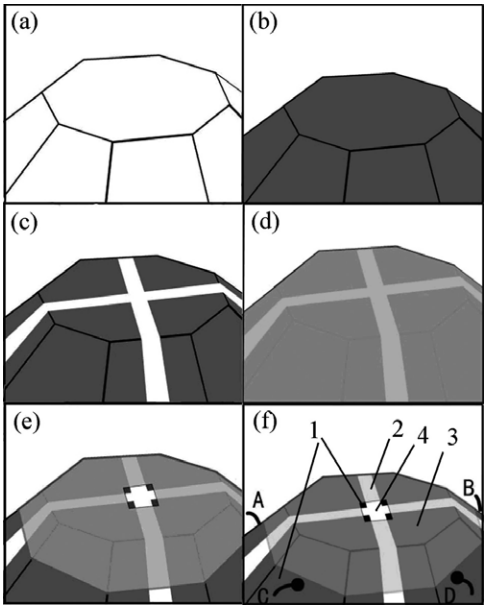

Figure 1. Manufacturing process and configuration of a microcircuit on a diamond anvil. (a) A diamond anvil. (b) An Mo film was deposited on the diamond anvil. (c) The Mo film was patterned by photolithography into four detecting electrodes according to van der Pauw's model. (d) An Al_2O_3 layer was sputtered on the patterned Mo film. (e) A part of the Al_2O_3 layer was removed to allow the required exposure. (f) The configuration of a complete microcircuit: 1 is the Mo electrodes; 2 is the Al_2O_3 layer deposited on the diamond anvil; 3 is the Al_2O_3 layer deposited on the Mo film; 4 is the exposed diamond anvil. A, B, C and D are four contact ends of the microcircuit.

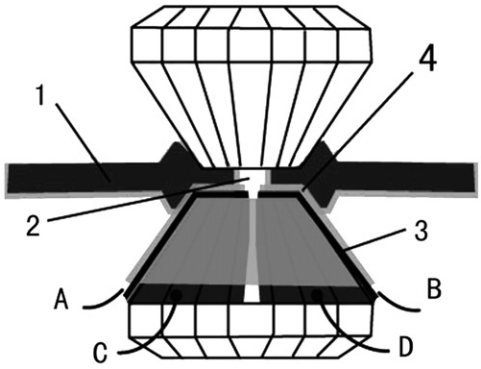

Figure 2. The cross section of the designed diamond anvil cell device: 1 is the gasket; 2 is the sample chamber; 3 is the Mo electrodes; 4 is the alumina layer. A, B, C and D are four contact ends of the microcircuit.

3. Results and discussion

3.1. Raman spectra under high pressure

Figure 3(a) shows the Raman spectra of $PbMoO_4$ recorded during a compression process. Five Raman vibration modes at ambient pressure can be seen. By comparison with the spectra

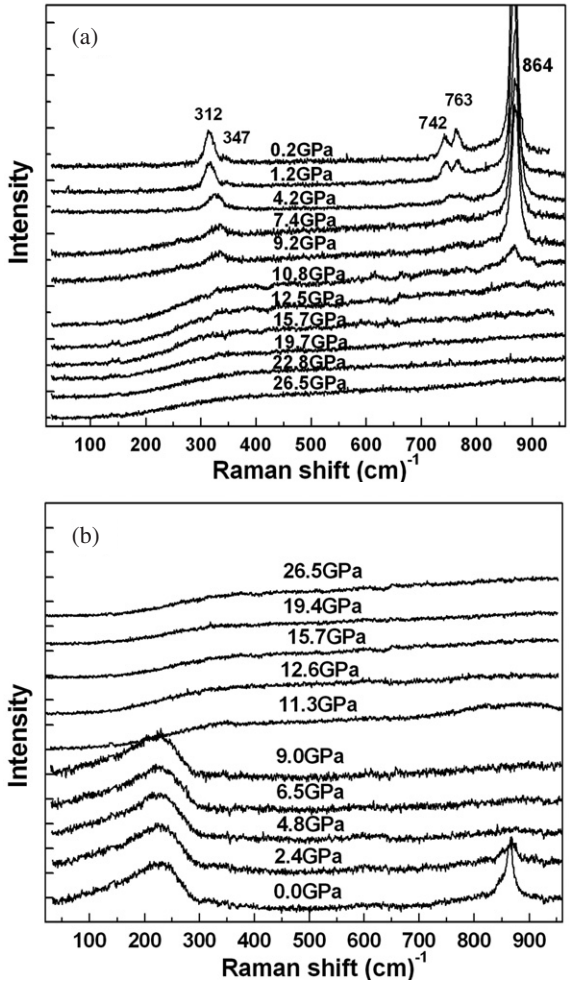

Figure 3. Raman spectra of $PbMoO_4$ recorded during the course of a compression (a) and a decompression (b).

of other molybdates [16–18], the modes centered at 864, 763 and 742 cm^{-1} are assigned to asymmetric stretching of MoO_4 tetrahedra and the 347 and 312 cm^{-1} modes are assigned to MoO_4 symmetric bending and asymmetric bending, respectively. With increasing pressure, the intensity of the Raman peaks decreased gradually. The Raman peak at 347 cm^{-1} almost disappears at 4.2 GPa. When the pressure increases to 7.4 GPa, the peaks at 742 and 763 cm^{-1} disappear. On increasing the pressure further to 10.8 GPa, the highest-frequency stretching mode starts to lose its sharpness (linewidth of $\sim$10 cm^{-1}) and it develops an excessive broadening (linewidth of $\sim$54 cm^{-1}). This anomalous broadening is due to a breakdown in the translational symmetry of the system. This is similar to the broad MoO_4 Raman mode observed at high pressure in amorphouse $Sc_2(MoO_4)_3$, $Eu_2(MoO_4)_3$ and $ZrMo_2O_8$ [19–21]. The similarity is reasonable, since they have a close structure with a very flexible framework due to the corner-shared tetrahedra configuration. Once pressure increases to 12.5 GPa, all Raman peaks completely disappeared. This suggests that the $PbMoO_4$ experiences a transformation from an ordered state to a disordered state between 9.2 and 12.5 GPa, i.e. pressure has induced

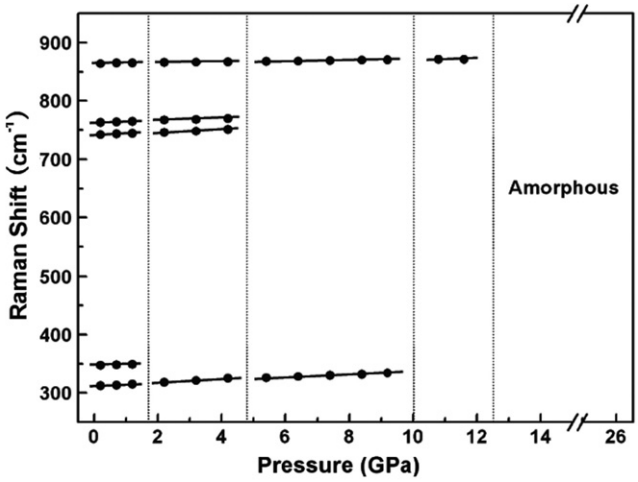

Figure 4. Pressure dependence of the Raman modes of $PbMoO_4$ during the compression process.

an amorphization process. The main changes observed in the spectrum can be followed by analyzing the frequency ω versus pressure P plot shown in figure 4. The results indicate that the material experiences structural modification at about $P = 1.7, 4.8, 10.1$ and 12.5 GPa. All the peaks can be fitted well with a linear pressure dependence $\omega(P) = \omega_0 + \alpha P$.

When the pressure was decreased from 26.5 to 11.3 GPa, the Raman spectra did not show any change, as shown in figure 3(b). On decreasing the pressure further to 9.0 GPa, the disordering Raman peak appeared at a low frequency, which illustrates that the structural property of $PbMoO_4$ is transformed in the course of decompression from 11.3 to 9.0 GPa. This origin of the disordering Raman peak is not yet clear and warrants further investigation, and a related study is underway. When the pressure was decreased to 2.4 GPa, only the peak at 864 cm^{-1} came back, which indicates that the phase transformation of $PbMoO_4$ under high pressure is incompletely reversible. This may be due to nonhydrostatic conditions in the DAC.

In molybdate compounds, the initial crystalline order may break down along three different mechanisms, namely (a) chemical decomposition, (b) mechanical deformation and (c) crystallographic transformation [20]. The first mechanism is decomposition of an initially complex compound into simpler components, which would destroy the original symmetry of samples. Irreversibility of the transformation, on the other hand, is consistent with chemical decomposition, as high-energy barriers prevent the reverse process (synthesis from the oxides) from taking place. However, the phase transformation of $PbMoO_4$ under high pressure is partially reversible, so the amorphization of $PbMoO_4$ cannot be illuminated by chemical decomposition. Furthermore, the mechanical process implies a nonhomogeneous macroscopic deformation of a crystalline sample by nonhydrostatic shear components, because there are pressure gradients in the diamond anvil cell under nonhydrostatic conditions and the shearing force applied to a sample is very large. Whereas the short-range chemical order, which existed in the original crystal unit cell, is preserved, the original symmetry of the crystals is gradually destroyed with an increase in pressure and finally amorphization occurs. The original symmetry of crystals recurred on release from high pressure. In addition, the crystallographic mechanism leads to a disorder in the crystal structure, both orientational and positional, but without any substantial atomic displacements or diffusion, and without any change in the initial chemical composition. Nonhydrostatic stress components, due to their symmetry properties, can be conjugated (coupled) to the elastic order parameter [22]. Such a selective resonance-type

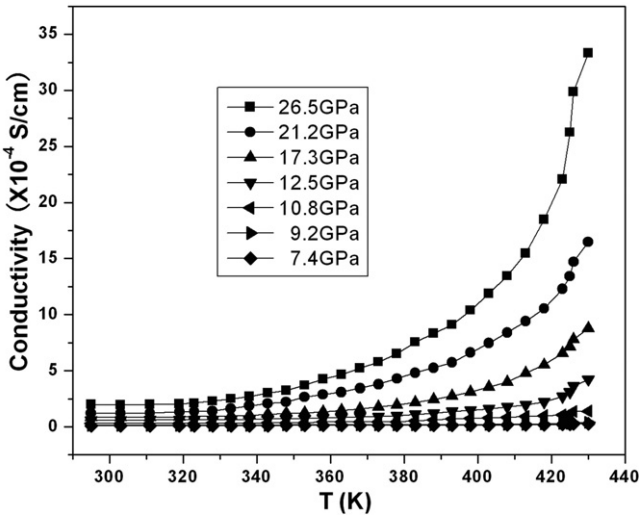

Figure 5. Electrical conductivity of $PbMoO_4$ as a function of temperature under various pressures.

coupling between the nonhydrostatic stress components and order parameter components can induce, in turn, the onset of a lattice shear instability, triggering the amorphization of the crystal [22]. Therefore, the amorphization of $PbMoO_4$ may be interpreted by the mechanical scenario and the crystallographic mechanism.

3.2. Electrical conductivity under high pressure and moderate temperature

Electronic transport is greatly sensitive to the crystal structure, which is easily distorted, especially under additional pressure. Moreover, electrical conduction in a semiconductor depends intensively on temperature, because the concentration of carriers in a semiconductor increases remarkably with increasing temperature.

Figure 5 shows the electrical conductivity of $PbMoO_4$ as a function of temperature under various pressures. It was found that the electrical conductivity of $PbMoO_4$ increased with increasing pressure and temperature. The means that, the higher the pressure and temperature is, the larger the electrical conductivity is. $PbMoO_4$ usually has a high resistivity at ambient pressure and temperature, and the electrical conductivity values of $PbMoO_4$ exceed our measurement range. $PbMoO_4$ usually has high resistivity at ambient pressure and room temperature; no potential difference was detected below 7.4 GPa within the measurement accuracy. At 7.4 and 9.2 GPa, the electrical conductivity values of $PbMoO_4$ were very low and not obviously changed by an increase in temperature. This is related to the intrinsic property of the material and is under further investigation. With increasing pressure up to 12.5 GPa, the electrical conductivity dependence of temperature becomes obvious, especially at higher pressure. At 430 K, the values of electrical conductivity of $PbMoO_4$ at 26.5 GPa increased by about two orders of magnitude compared to that at 7.4 GPa. As seen from Raman spectra during the compression run, $PbMoO_4$ experienced a transformation from crystal to amorphous phase gradually between 9.2 and 12.5 GPa. When the pressure is over 12.5 GPa, $PbMoO_4$ is amorphous. For amorphization, a lot of defect energy levels would appear among energy bands, which is favorable for electrons hopping from the valence band to the conductive band. In addition, the degree of electronic cloud overlap was enhanced with increasing pressure, reducing the electron hopping distance. The higher the pressure and temperature, the easier

the electron hopping from valence band to conductive band. Thus the concentration of carriers increases, which results in an increase in the electrical conductivity of $PbMoO_4$.

4. Conclusion

In summary, the high-pressure Raman spectrum of $PbMoO_4$ was determined up to 26.5 GPa in a diamond anvil cell. During the course of compression, the $PbMoO_4$ gradually experienced a transformation from crystal to amorphous phase between 9.2 and 12.5 GPa. The crystal-to-amorphous phase transition may be due to the mechanical deformation and crystallographic transformation. When pressure was released, the structural phase transformation of $PbMoO_4$ is incompletely reversible. The electrical conductivity of $PbMoO_4$ was measured accurately *in situ* using a microcircuit fabricated on a DAC based on the van der Pauw method. The results show that the electrical conductivity of $PbMoO_4$ increases with increasing pressure and temperature. The effect of pressure on the electrical conductivity of $PbMoO_4$ is more obvious than that of temperature.

Acknowledgments

This work was supported by the National Natural Science Foundation of China (grant nos 40473034, 10574055 and 50532020) and the National Basic Research Program of China (grant no. 2005CB724404).

References

[1] Pinnow D A, Uitert I G V and Warner A W 1969 *Appl. Phys. Lett.* **15** 83
[2] Boneer W A and Dzik G J 1970 *J. Cryst. Growth* **7** 65
[3] Coquin G A, Pinnow D A and Warner A W 1971 *J. Appl. Phys.* **42** 2162
[4] Satoh T, Ohhara A, Fujii N and Namikata T 1974 *J. Cryst. Growth* **24/25** 441
[5] Takano S, Esashi S, Mori K and Namikata T 1974 *J. Cryst. Growth* **24/25** 437
[6] Minowa M, Itakura K, Moriyama S and Ootani W 1992 *Nucl. Instrum. Methods* **320** 500
[7] Zeng H C 1997 *J. Cryst. Growth* **171** 136
[8] Spasskya D A, Ivanov S N, Kolobanov V N, Mikhailin V V, Zemskov V N, Zadneprovski B I and Potkin L I 2004 *Radiat. Meas.* **38** 607
[9] Ganguly B N and Nicol M 1977 *Phys. Status Solidi* b **79** 617
[10] Jayaraman A, Batlogg B and VanUitert L G 1985 *Phys. Rev.* B **31** 8
[11] Van Loo W 1975 *J. Solid State Chem.* **14** 359
[12] Groenink J A and Binsma H 1979 *J. Solid State Chem.* **29** 227
[13] Volnyanskiĭ M D, Kudzin A Y, Plyaka S N and Balasme Z 2004 *Phys. Solid State* **46** 2012
[14] Gao C, Han Y, Ma Y, White A, Liu H, Luo J, Li M, He C, Hao A, Huang X, Pan Y and Zou G 2005 *Rev. Sci. Instrum.* **76** 083912
[15] Han Y, Gao C, Ma Y, Liu H, Pan Y, Luo J, Li M, He C, Huang X, Zou G, Li Y, Li X and Liu J 2005 *Appl. Phys. Lett.* **86** 064104
[16] Maczka M 1997 *J. Solid State Chem.* **129** 287
[17] Augsburger M S and Pedregosa J C 1994 *J. Phys. Chem. Solids* **56** 1081
[18] Jayaraman A, Wang S Y and Sharma S K 1995 *Solid State Commun.* **93** 885
[19] Paraguassu W, Maczka M, Souza Filho A G, Freire P T C, Mendes Filho J, Melo F E A, Macalik L, Gerward L, Staun Olsen J, Waskowska A and Hanuza J 2004 *Phys. Rev.* B **69** 094111
[20] Vladimir D, Vitaly S, Ruben D, Denis M, Alexey K, Eugeny P, Guy L and Hans P W 2003 *J. Phys. Chem. Solids* **64** 307
[21] Muthu D V S, Chen B, Wrobel J M, Krogh Andersen A M, Carlson S and Kruger M B 2002 *Phys. Rev.* B **65** 064101
[22] Binggeli N and Chelikowsky J R 1992 *Phys. Rev. Lett.* **69** 2220